Crystallization behavior of SiO2-P2O5-CaO-MgO-Na2O-K2O bioactive glass powder

Research Article

Elisa Fiume, Enrica Verné, and Francesco Baino*

Crystallization behavior of SiO_2–P_2O_5–CaO–MgO–Na_2O–K_2O bioactive glass powder

https://doi.org/10.1515/bglass-2019-0004
Received Nov 12, 2018; revised Mar 05, 2019; accepted May 04, 2019

Abstract: The crystallization process of a bioactive silicate glass with $47.5SiO_2$-$10Na_2O$-$10K_2O$-10MgO-20CaO-$2.5P_2O_5$ molar composition was investigated by using non-isothermal differential thermal analysis (DTA). The DTA plots recorded at different heating rates exhibited a single crystallization peak. The activation energy for crystallization was estimated by applying the equations proposed by Kissinger and Matusita-Sakka. The Johnson-Mehl-Avrami exponent (n) was assessed by using the Ozawa and Augis-Bennett methods. The analyses suggest that a surface crystallization mechanism with one-dimensional crystal growth is predominant. The activation energy for viscous flow was also assessed (176 kJ/mol) and was found lower than the activation energy for crystallization (271 kJ/mol). This confirms the stability of 47.5B against crystallization and its good sinterability, which is a highly attractive feature for producing glass products of biomedical interest, such as bioactive porous scaffolds for bone repair.

Keywords: Bioactive glass; Glass-ceramic; Thermal analysis; Crystallization

1 Introduction

Bioactive glasses were invented fifty years ago at the University of Florida by Prof. Larry Hench and his team, who developed the famous 45S5 composition ($45SiO_2$-24.5CaO-$24.5Na_2O$-$6P_2O_5$ wt.%) [1]. This glass, trade-named as Bioglass®, was initially found able to bond both to bone and to soft collagenous tissues of the body [2]. Hence, it was soon considered an excellent biomaterial to repair bone tissue undergoing injury or dysfunctionality and, to date, it has been implanted in more than 1.5 million patients suffering from osseous defects in orthopedic and dental applications [3]. Recent studies carried out over the past two decades have also revealed additional highly-appealing properties of 45S5 Bioglass®, including an inherent antibacterial effect due to the release of alkaline ions (Ca^{2+} and Na^{+}) [4, 5] and the capability to stimulate angiogenesis, which is the key to accelerate wound healing process [6, 7].

The main drawback of 45S5 Bioglass® concerns its poor workability: in fact, the glass transition temperature (T_g) and the onset of crystallization (T_x) are very close, thus limiting the possibility of sintering by viscous flow [8]. As a result, 45S5 glass cannot be sintered without undergoing devitrification, which has an impact on the kinetics of apatite formation (bioactivity) *in vitro* and *in vivo* and, hence, on the bone-bonding capability and osteointegration rate. In this regard, Peitl *et al.* [9] showed that the onset time of hydroxyapatite formation on the surface of 45S5 Bioglass® increases from 8 to 25 h when the crystalline fraction increases from 0 to 60%; however, the bioactivity is not totally suppressed and the partially-crystallized material is still potentially suitable for biomedical applications [10–12]. A similar behavior was also found to occur in other silicate (*e.g.* S53P4, $53SiO_2$-$20CaO$-$23Na_2O$-$4P_2O_5$ wt.% [13]) and phosphate glasses ($50P_2O_5$-(40 – x)CaO-xSrO-$10Na_2O$ with x = 0, 20, and 40 mol.%) [14]. Over the years, other glasses have been developed with a larger sintering window (*e.g.* 13-93, $53SiO_2$-$6Na_2O$-$12K_2O$-5MgO-20CaO-$4P_2O_5$ wt.%) [15] and/or with the capability of retaining an excellent and fast apatite-forming ability also in partially-crystallized forms (*e.g.* CEL2, $43.8SiO_2$-$15.0Na_2O$-$6.1K_2O$-4.6MgO-23.6CaO-$6.9P_2O_5$ wt.%) [16].

The fabrication of sintered bioactive glass products, such as three-dimensional macroporous scaffolds, is often a challenge because, on one hand, extensive densifica-

***Corresponding Author: Francesco Baino:** Institute of Materials Physics and Engineering, Applied Science and Technology Department, Politecnico di Torino, Corso Duca degli Abruzzi 24, 10129 Torino, Italy; Email: francesco.baino@polito.it; Tel.: +39 011 090 4668; Fax: +39 011 090 4624
Elisa Fiume, Enrica Verné: Institute of Materials Physics and Engineering, Applied Science and Technology Department, Politecnico di Torino, Corso Duca degli Abruzzi 24, 10129 Torino, Italy

tion is required to achieve enough strength for the glass-derived product to be safely handled and, on the other hand, crystallization of the glass, which could negatively affect the bioactivity, may occur prior to significant densification.

Amorphous scaffolds made of sintered 13-93 glass were reported to have suitable mechanical properties for bone repair applications, but their apatite-forming ability was lower compared to 45S5 composition [17]. A comparative study between CEL2- and 45S5-derived glass-ceramic foams suggested that the apatite-forming kinetics of the former are faster, leading to a thicker surface layer of hydroxyapatite [18].

Verné *et al.* developed a silicate glass (47.5B) with an exceptionally large sinterability range ($T_x - T_g = 260°C$) and retaining *in vitro* bioactivity after partial devitrification at 800°C for 3 h [19]. These properties suggest the potential suitability of such a material for making bioactive porous scaffolds; however, the crystallization behavior should be determined first. In this regard, the present work aims at investigating the crystallization mechanism of 47.5B glass powder under non-isothermal conditions in order to assess the activation energies for crystallization and viscous flow. These parameters have not been determined for such glass composition so far. Over the past half century, a number of approaches have been developed to estimate the activation energy for crystallization [20], but there is a paucity of relevant studies about biomedical glasses. Of those, the vast majority focused on 45S5 Bioglass® [21, 22], while almost no information have been provided on other bioactive glass systems.

2 Materials and methods

2.1 Glass preparation

The analyzed material was a glass (47.5B) originally developed by Verné *et al.* [19] at Politecnico di Torino in the composition 47.5SiO_2-10Na_2O-10K_2O-10MgO-20CaO-2.5P_2O_5 (mol.%) and was produced using a standard melting method in a platinum crucible. The raw precursors (SiO_2, Na_2CO_3, K_2CO_3, $(MgCO_3)_4{\cdot}Mg(OH)_2{\cdot}5H_2O$, $CaCO_3$ and $Ca_3(PO_4)_2$ high-purity powders purchased from Sigma-Aldrich) were homogeneously mixed in the crucible and melted in air at 1500°C for 0.5 h; the melt was then quenched in deionized water to produce a frit that was ball milled (Pulverisette 0, Frtisch, Germany) and sieved below 32 µm by a stainless steel sieve (Giuliani Technologies Srl, Torino, Italy). According to the authors' previous experience on other glass compositions, this particle size range is very suitable to produce porous glass-derived scaffolds by various technologies, including foam replication and robocasting; this is the reason why the glass crystallization behavior was studied using 47.5B powder with such size.

2.2 Thermal properties

The glass transition temperature (T_g) and the peak crystallization temperature (T_p) were determined by differential thermal analysis (DTA; DTA404PC, Netzsch, Germany) at various heating rates β (10, 20, 30 and 40°C/min). The measurements were performed on 50 mg of glass that was heated to 1200°C in a platinum crucible under nitrogen flow (inert atmosphere) using Al_2O_3 powder as a reference material. The glass transition temperature was determined at the inflection point of the DTA curve, as obtained from the first derivative of the thermal plot. The peak crystallization temperature was found at the maximum of the exothermic peak. The accuracy of the measurements was ± 3°C.

2.3 Analysis of the crystallization process

The crystallization process in glasses is usually described by two parameters, *i.e.* the Johnson-Mehl-Avrami (JMA) coefficient (n) – which depends on the mechanism of crystal nucleation and growth [23, 24] – and the activation energy for crystallization.

The JMA coefficient was quantified by suing two independent techniques. First, it was determined by the Ozawa equation [25]:

$$-n = \left.\frac{d\left(\ln\left(-\ln\left(1-\chi\right)\right)\right)}{d(\ln\beta)}\right|_T \quad (1)$$

where χ is the volume fraction of crystallized phase at a fixed temperature T. The values of χ were estimated from the DTA plots as the ratio between the partial area under the exothermic peak (at a chosen temperature) and the total area under the peak. A plot of $\ln(-\ln(1-\chi))$ vs. $\ln\beta$, followed by linear interpolation, gives a straight line of slope n. The value of the JMA parameter n was calculated as mean ± SD of the slopes of the plots.

The coefficient n was also estimated by using the Augis-Bennet method [26]:

$$n = \frac{2.5RT_p^2}{\Delta T_{FWHM}E_c} \quad (2)$$

where ΔT_{FWHM} is the full width of the DTA exothermic peak at the half maximum. In this case, the JMA parameter

was calculated as mean ± SD of the n-values determined at each heating rate (β).

The activation energy for crystallization can be assessed from non-isothermal DTA data by applying models that relate the variation of T_p to the heating rate β. Kissinger proposed the following equation to estimate the crystallization activation energy ($E_{c,K}$) [27]:

$$\ln \frac{\beta}{T_p^2} = -\frac{E_{c,K}}{RT_p} + constant \quad (3)$$

A plot of $\ln \frac{\beta}{T_p^2}$ vs. $\frac{1}{T_p}$, followed by linear interpolation, gives a straight line of slope $\frac{E_{c,K}}{R}$ (R = 8.314 J/mol K is the ideal gas constant), from which $E_{c,K}$ can be easily calculated.

However, Matusita *et al.* [28] demonstrated that Equation (3) is valid only when crystal growth occurs on a fixed number of nuclei. Hence, the Kissinger model yields an underestimated value of the activation energy for crystallization if most nuclei are formed during the DTA measurement, as the number of nuclei may vary with β. A more general equation deriving from the Kissinger model was then proposed by Matusita and Sakka [29]:

$$\ln \frac{\beta^n}{T_p^2} = -\frac{mE_c}{RT_p} + constant \quad (4)$$

where E_c is the correct activation energy for crystallization, n is the JMA exponent and m is a numerical factor which depends on the dimensionality of crystal growth, *i.e.* three-dimensional sphere-like (m = 3), two-dimensional plate-like (m = 2) or one-dimensional rod-like (m = 1) crystallization [30]. A plot of $\ln \frac{\beta^n}{T_p^2}$ vs. $\frac{1}{T_p}$, followed by linear interpolation, gives a straight line of slope $\frac{mE_c}{R}$, from which E_c can be calculated.

As a general rule, we have m ≈ 1 when surface crystallization predominates, whereas m ≈ 3 when bulk crystallization is predominant. The value of m is related to n as m = n − 1 when crystal nucleation occurs during DTA. When a surface crystallization mechanism is dominant, we have m = n = 1 regardless of whether nuclei are formed prior to or during thermal analysis: in this case, Matusita-Sakka equation (Equation (4)) essentially reduces to the Kissinger one (Equation (3), *i.e.* $E_c = E_{cK}$ [30].

The activation energy for viscous flow (E_{vf}) was estimated by following the approach proposed by Francis *et al.* [31] who suggested the application of a Kissinger-type model. Thus, a plot of $\ln \frac{\beta}{T_g^2}$ vs. $\frac{1}{T_g}$, followed by linear interpolation, gives a straight line of slope $\frac{E_{vf}}{R}$, from which E_{vf} can be easily calculated.

The validity of the JMA model was discussed by using the method proposed by Malek [24]. He showed that, for the model to be applicable, the crystallization rate $\frac{d\chi}{dt}$ must depend only on the fraction χ of the glass crystallized and the temperature T, *i.e.* the thermal history of the material must not affect the crystallization mechanism. This validity test is based on the analysis of a probe function $z(\chi) \propto \frac{d\chi}{dt}$, which in non-isothermal conditions is defined as:

$$z(\chi) = \phi T^2 \quad (5)$$

where ϕ is the specific heat flow.

According to the Equation (5), the function $z(\chi)$ does not depend on kinetic parameters, and the JMA model is valid if the maximum of $z(\chi)$ is located at $\chi = 0.63 \pm 0.02$ [32].

3 Results and discussion

Figure 1 shows the DTA plots of 47.5B glass powder at different heating rates. A single exothermic peak of crystallization was recorded, which is consistent with previous investigations on this glass system [19]. The glass transition and peak crystallization temperatures can be observed to increase as the heating rate β increases from 10 to 40°C/min. Specifically, T_g and T_p vary within 527-567°C and 765-848°C, respectively.

The JMA coefficient n was initially calculated from the Ozawa plots at five different temperatures (770, 780, 790, 800 and 810°C) (Figure 2) and found equal to 1.4 ± 0.03. Assessment of n by the Augis-Bennet method yielded the value 1.8 ± 0.2, which is comparable to the Ozawa's one.

Figure 3 shows the Kissinger plot for the calculation of $E_{c,K}$; the least squares fitting yielded an apparent activation energy for crystallization of 131 kJ/mol. However, since both the Ozawa model and the Augis-Bennet method yield a value of n > 1, the application of the Kissinger equation is not appropriate and could lead to an underestimation of the activation energy. As the crystal growth dimensionality m can be calculated as n − 1 in the case of a non-constant number of nuclei, which happens during the DTA experiments while crystal nucleation occurs, we can assume that m is approximately equal to 1 [33, 34]. This value indicates that surface crystallization is dominant with one-dimensional rod-like crystallization in 47.5B glass particles. Once the values of n and m have been calculated, it is possible to apply the equation proposed by Matusita and Sakka (Equation (4)) [29] to calculate the activation energy for crystallization in a more reliable way as compared to the Kissinger model. The relevant plot is reported in Figure 4 and yielded an energy value E_c of 251 kJ/mol (> $E_{c,K}$).

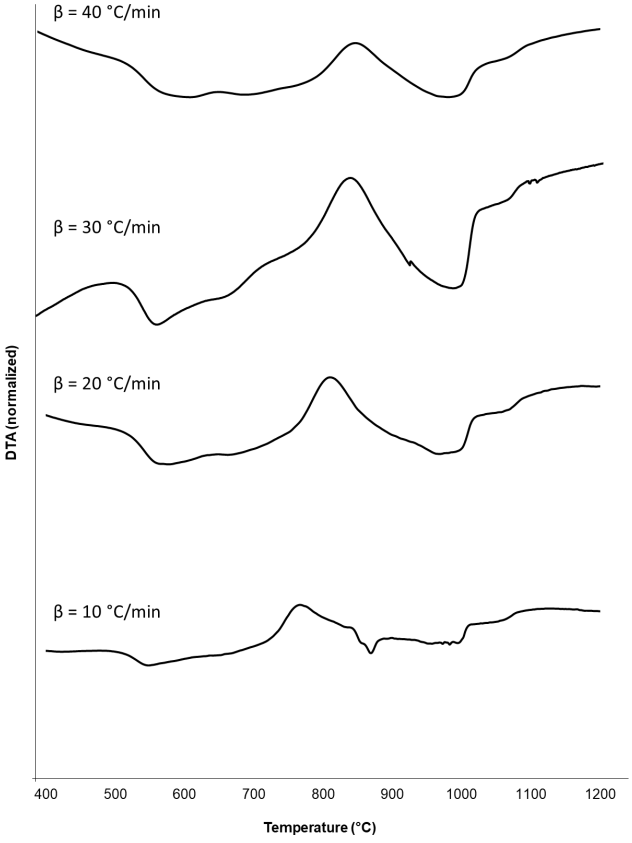

Figure 1: DTA thermographs of 47.5B glass powders collected at different heating rates (β).

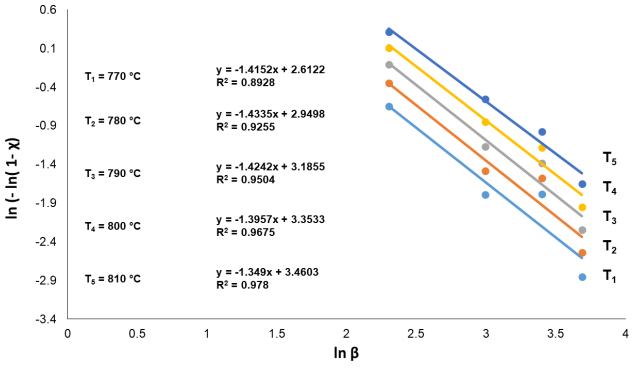

Figure 2: Plots in accordance with the Ozawa equation to determine the JMA parameter (n).

Erol *et al.* [35] suggested a simplified approach to calculate E_c starting from the (incorrect) value of $E_{c,K}$ when $m \neq n \neq 1$. Equations (3) and (4) can be combined together to obtain the following formula:

$$E_c = \frac{n}{m}E_{c,K} - 2\frac{n-1}{m}RT_p \quad (6)$$

As the condition $E_c >> 20RT_p$ is verified in most oxide glass systems [36], the term $2\frac{n-1}{m}RT_p$ in Equation (6) can be eliminated introducing an error of less than 10% in the value of

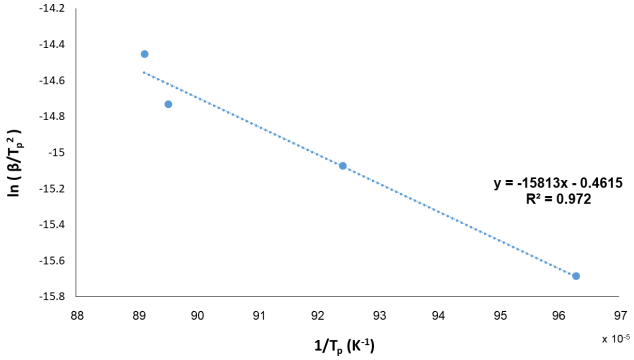

Figure 3: Plot in accordance with the Kissinger equation to determine the apparent activation energy for crystallization (E_{cK}).

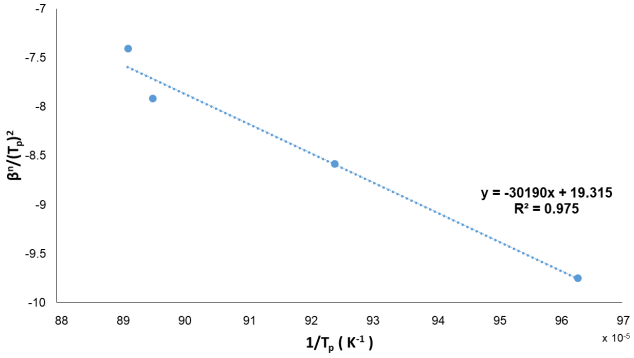

Figure 4: Plot in accordance with the Matusita and Sakka equation to determine the correct activation energy for crystallization (E_c).

E_c. Hence, the following simple relation can be obtained:

$$E_c \approx \frac{n}{m}E_{c,K} \quad (7)$$

The activation energy for crystallization obtained by Equation (7) is 236 kJ/mol, which actually differs by only 6.4 % from the value assessed by Matusita-Sakka interpolation (251 kJ/mol) (Figure 4).

It is interesting to observe that the value of E_c for 47.5B glass powder assessed in this study is lower than that observed for powder of classical 45S5 Bioglass® with the same particle size range below 32 µm (*e.g.* 311 kJ/mol in [37] and 381-399 kJ/mol in [22]); a comparison of the relevant parameters is shown in Table 1. This depends on the different glass formulations and, hence, on the bonding energies involved. Because of the high bonding strengths of Si–O and P–O bonds, it is unlikely that a significant number of these bonds is broken during devitrification; rather, as suggested by Clupper and Hench [21], crystallization is expected to involve the breaking of modifier–O bonds that may have bonding strengths lower than E_c. In particular, K–O bonds having a significantly low bonding energy [38] are present in 47.5B glass and absent in 45S5 Bioglass®, which suggests that the former may require a compara-

Table 1: Thermal and kinetic parameters of 47.B and 45S5 Bioglass® particles.

Glass powder (<32 µm)	n	m	E_c (kJ/mol)	E_{vf} (kJ/mol)	K_H [a]
47.5B	1.4-1.8	1	251	181	0.40
45S5 Bioglass®	1 [22, 37]	1 [22, 37]	311 [37], 381-399 [22]	338 [37]	0.066 [16]

[a] The Hruby parameter was determined using a heating rate β = 20 °C/min in the DTA experiment, with T_g = 542°C, T_x = 670°C and T_m = 990°C.

tively lower activation energy for crystallization. Furthermore, it is worth observing that the crystalline phases formed during devitrification of the two materials are different, and this could also justify the different values of E_c. In fact, 47.5B tends to crystallize to $Na_2CaSi_3O_8$ after thermal treatment at 800°C [19], whereas other phases were reported to develop in 45S5 Bioglass®. In this regard, phase assignment of crystallized 45S5 Bioglass® is not unanimous. Over the years, different research groups suggested different possible scenarios, *i.e.* crystallization of $Na_2Ca_2Si_3O_9$ [9, 21] or $Na_2CaSi_2O_6$ [8, 15] as the main phase, with the optional presence of $Na_2Ca_4(PO_4)_2SiO_4$ (silicorhenanite) as a secondary phase [39]. In the attempt to solve this controversy Bellucci *et al.* [40] hypothesized the coexistence of $Na_2Ca_2Si_3O_9$and $Na_2CaSi_2O_6$, but this topic is still under debate.

It is also interesting to highlight that previous SEM observations on partially-devitrified 47.5B glass revealed the needle-like morphology of $Na_2CaSi_3O_8$ crystals [19], which is in agreement with the dimensionality of crystal growth (m = 1, one-dimensional rod-like) assessed in this work.

The Kissinger-type plot used for estimating the viscous flow activation energy is shown in Figure 5 and the least squares interpolation yields a value of 181 kJ/mol. E_{vf} is lower than E_c, showing that the energy needed for viscous flow to occur is lower than that required for diffusion to progress the crystallization. This confirms that 47.5B glass exhibits a higher stability against crystallization as compared to 45S5 Bioglass®, which conversely has $E_c < E_{vf}$ (Table 1) and a rapid tendency to crystallize just above T_g [37].

This behavior can be further quantified by calculating the Hruby parameter that is defined as follows [41]:

$$K_H = \frac{T_x - T_g}{T_m - T_x} \quad (8)$$

where T_x is the onset of crystallization and T_m the melting temperature determined from DTA plot.

The Hruby parameter K_H serves as a measure of the glass stability against crystallization: the larger K_H of a certain glass, the greater its stability against crystallization upon heating [42]. As shown in Table 1, the Hruby parameter of 47.5B glass (0.40) is six times higher than that calculated for 45S5 Bioglass® powder (0.066) [16] under the same experimental conditions.

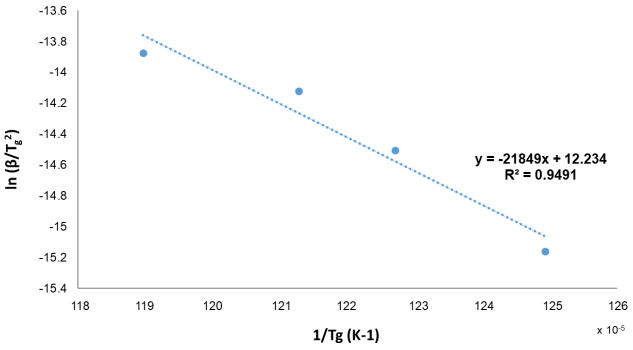

Figure 5: Kissinger-type plot for the determination of the activation energy for the viscous flow (E_{vf}).

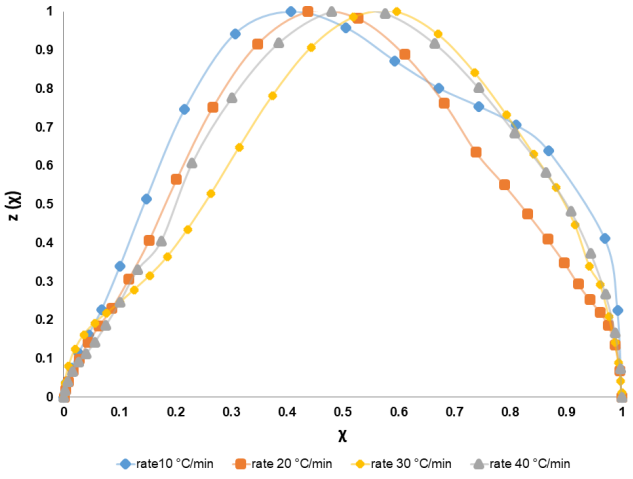

Figure 6: Plots of the normalized z(χ) functions (Malek test).

The JMA model validity was assessed by applying the method proposed by Malek [24]. The normalized z(χ) functions, reported in Figure 6, have a typical bell-type shape and their maximum varies from 0.40 to 0.48 as the hating rate β increases from 10 to 40°C/min. Therefore, the crystallization process of 47.5B bioactive glass can be just approximately described by the JMA model, which is valid only if the maximum of the z(χ) function is located at χ = 0.63 ± 0.02 [32]. This suggests that the crystallization mechanism in 47.5B glass is more complex than a simple process of crystal nucleation and growth and may also change as a function of the heating rate. Future investigations could

be addressed to elucidate whether, for example, glass-in-glass phase separation takes place during the crystallization of 47.5B, as observed in other bioactive glass systems such as 45S5 Bioglass® [8, 22, 43].

4 Conclusions

This work investigated the crystallization process of a SiO_2–P_2O_5–CaO–MgO–Na_2O–K_2O bioactive glass under non-isothermal conditions. The analyses gave evidence of a complex crystallization process where surface crystallization associated to the development of rod-like crystals was dominant. The activation energy for viscous flow was found lower than that required for crystallization, which suggests the capability of this glass to achieve significant densification before crystallization begins when it is thermally-treated above T_g. From a methodological viewpoint, this study also demonstrates that using multiple and complementary methods, *i.e.* the Ozawa and Augis-Bennet methods for determining the JMA exponent n as well as the Kissinger and Matusita-Sakka equations for assessing the crystallization activation energy, is fundamental to accurately describe the crystallization parameters.

References

[1] Hench L.L., Splinter R.J., Allen W.C., Greenlee T.K., Bonding Mechanisms at the Interface of Ceramic Prosthetic Materials, J Biomed Mater Res 1971, 5, 117-141.

[2] Wilson J., Pigott G.H., Schoen F.J., Hench L.L., Toxicology and Biocompatibility of Bioglasses, J Biomed Mater Res 1981, 15, 805-817.

[3] Jones J.R., Brauer D.S., Hupa L., Greenspan D.C., Bioglass and Bioactive Glasses and Their Impact on Healthcare, Int J Appl Glass Sci 2016, 7, 423-434.

[4] Hu S., Chang J., Liu M., Ning C, Study on Antibacterial Effect of 45S5 Bioglass. J Mater Sci Mater Med 2009, 20, 281-286.

[5] Begum S., Johnson W.R., Worthington T., Martin R.A., The Influence of pH and Fluid Dynamics on the Antibacterial Efficacy of 45S5 Bioglass, Biomed Mater 2016, 11, 015006.

[6] Gerhardt L.C., Widdows K.L., Erol M.M., Burch C.W., Sanz-Herrera J.A., Ochoa I., Stämpfli R., Roqan I.S., Gabe S., Ansari T., Boccaccini A.R., The Pro-Angiogenic Properties of Multi-Functional Bioactive Glass Composite Scaffolds, Biomaterials 2011, 32, 4096-4108.

[7] Handel M., Hammer T.R., Nooeaid P., Boccaccini A.R., Hoefer D., 45S5-Bioglass®-Based 3D-Scaffolds Seeded with Human Adipose Tissue-Derived Stem Cells Induce In Vivo Vascularization in the CAM Angiogenesis Assay, Tissue Eng A 2013, 19, 2703-2712.

[8] Lefebvre L., Chevalier J., Gremillard L., Zenati R., Thollet G., Bernache-Assolant D., Govin A., Structural Transformations of Bioactive Glass 45S5 with Thermal Treatments, Acta Mater 2007, 55, 3305-3313.

[9] Peitl O., LaTorre G.P., Hench L.L., Effect of Crystallization on Apatite Layer Formation of Bioactive Glass 45S5, J Biomed Mater Res 1996, 30, 509-514.

[10] Leonor I.B., Ito A„ Onuma K., Kanzaki N., Zhong Z.P., Greenspan D., Reis R.L., In Situ Study of Partially Crystallized Bioglass® and Hydroxylapatite In Vitro Bioactivity Using Atomic Force Microscopy. J Biomed Mater Res 2002, 62, 82-88.

[11] Plewinski M., Schickle K., Lindner M., Kirsten A., Weber M., Fischer H., The Effect of Crystallization of Bioactive Bioglass 45S5 on Apatite Formation and Degradation, Dent Mater 2013, 29, 1256-1264.

[12] Kashyap S., Griep K., Nychka J., Crystallization Kinetics, Mineralization and Crack Propagation in Partially Crystallized Bioactive Glass 45S5. Mater Sci Eng C 2011, 31, 762-769.

[13] Fagerlund S., Massera J., Moritz N., Hupa L., Hupa M., Phase Composition and In Vitro Bioactivity of Porous Implants Made of Bioactive Glass S53P4, Acta Biomater 2012, 8, 2331-2339.

[14] Massera J., Mayran M., Rocherullé J., Hupa L., Crystallization Behavior of Phosphate Glasses and Its Impact on the Glasses' Bioactivity, J Mater Sci 2015, 50, 3091-3102.

[15] Fu Q., Saiz E., Tomsia A.P., Direct Ink Writing of Highly Porous and Strong Glass Scaffolds for Load-Bearing Bone Defects Repair and Regeneration, Acta Biomater 2011, 7, 3547-3554.

[16] Baino F., Ferraris M., Bretcanu O., Verné E., Vitale-Brovarone C., Optimization of Composition, Structure and Mechanical Strength of Bioactive 3-D Glass-Ceramic Scaffolds for Bone Substitution, J Biomater Appl 2013, 27, 872-890.

[17] Fu Q., Rahaman M.N., Bal B.S., Brown R.F., Day D.E., Mechanical and In Vitro Performance of 13–93 Bioactive Glass Scaffolds Prepared by a Polymer Foam Replication Technique, Acta Biomater 2008, 4, 1854-1864.

[18] Renghini C., Giuliani A., Mazzoni S., Brun F., Larsson E., Baino F., Vitale-Brovarone C., Microstructural Characterization and In Vitro Bioactivity of Porous Glass-ceramic Scaffolds for Bone Regeneration by Synchrotron Radiation X-ray Microtomography, J Eur Ceram Soc 2013, 33, 1553-1565.

[19] Verné E., Bretcanu O., Balagna C., Bianchi C.L., Cannas M., Gatti S., Vitale-Brovarone C., Early Stage Reactivity and In Vitro Behavior of Silica-Based Bioactive Glasses and Glass-Ceramics, J Mater Sci Mater Med 2009, 20, 75-87.

[20] Starink M.J., The Determination of Activation Energy from Linear Heating Rate Experiments: A Comparison of the Accuracy of Isoconversion Methods, Thermochim Acta 2003, 404, 163-176.

[21] Clupper D.C., Hench L.L., Crystallization Kinetics of Tape Cast Bioactive Glass 45S5, J Non-Cryst Solids 2003, 318, 43-48.

[22] Golovchak R., Thapar P., Ingram A., Savytskii D., Jain H., Influence of Phase Separation on the Devitrification of 45S5 Bioglass, Acta Biomater 2014,10, 4878-4886.

[23] Avrami M., Kinetics of Phase Change. I General Theory, J Chem Phys 1939, 7, 1103-1112.

[24] Malek J., Kinetic Analysis of Crystallization Processes in Amorphous Materials, Thermochim Acta 2000, 355, 239-253.

[25] Ozawa T., Kinetics of Non-Isothermal Crystallization, Polymers 1971, 12, 150-158.

[26] Augis J.A., Bennett J.E., Calculation of the Avrami Parameters for Heterogeneous Solid State Reactions Using a Modification of the Kissinger Method, J Thermal Anal 1978, 13, 283-292

[27] Kissinger H.E., Variation of Peak Temperature with Heating Rate in Differential Thermal Analysis, J Res Natl Bur Stand 1956, 57,

217-221.
[28] Matusita K., Sakka S., Matsui Y., Determination of the Activation Energy for Crystal Growth by Differential Thermal Analysis, J Mater Sci 1975, 10, 961-966.
[29] Matusita K., Sakka S., Kinetic Study of Crystallization of Glass by Differential Thermal Analysis - Criterion on Application of Kissinger Plot, J Non-Cryst Solids 1980, 38-39, 741-746.
[30] Matusita K., Komatsu T., Yokota R., Kinetics of non-isothermal crystallization process and activation energy for crystal growth in amorphous materials, J Mater Sci 1984, 19, 291-296.
[31] Francis A.A., Rawlings R.D., Sweeney R., Boccaccini A.R., Crystallization Kinetic of Glass Particles Prepared from a Mixture of Coal Ash and Soda-Lime Cullet Glass, J Non-Cryst Solids 2004, 333, 187-193.
[32] Malek J., Mitsuhashi T., Testing Method for the Johnson–Mehl–Avrami Equation in Kinetic Analysis of Crystallization Processes, J Am Ceram Soc 2000, 83, 2103-2105.
[33] Lilensten L., Fu Q., Wheaton B.R., Credle A.J., Stewart R.L., Kohli J.T., Kinetic study on Lithium-Aluminosilicate (LAS) Glass-Ceramics Containing MgO and ZnO, Ceram Int 2014, 40, 11657-11661.
[34] Smeacetto F., Radaelli M., Salvo M., Di Modugno D., Sabato A.G., Casalegno V., Broglia M., Ferraris M., Glass-Ceramic Joining Material for Sodium-Based Battery, Ceram Int 2017, 43, 8329-8333.
[35] Erol M., Kucukbayrak S., Ersoy-Mericboyu A., The Application of Differential Thermal Analysis to the Study of Isothermal and Non-Isothermal Crystallization Kinetics of Coal Fly Ash Based Glasses, J Non-Cryst Solids 2009, 355, 569-576.
[36] Yınnon H., Uhlmann D.R., Applications of Thermoanalytical Techniques to the Study of Crystallization Kinetics in Glass-Forming Liquids, Part I: Theory, J Non-Cryst Solids 1983, 54, 253-275.
[37] Baino F., Fiume E., Quantifying the Effect of Particle Size on the Crystallization of 45S5 Bioactive Glass, Mater Lett 2018, 224, 54-58.
[38] Luo Y.R., Comprehensive Handbook of Chemical Bond Energies, CRC Press, Boca Raton, FL (USA), 2007, pp. 1-1688.
[39] Bretcanu O., Chatzistavrou X., Paraskevpoulos K., Conradt R., Thompson I., Boccaccini A.R., Sintering and Crystallization of 45S5 Bioglass® Powder, J Eur Ceram Soc 2009, 29, 3299-3306.
[40] Bellucci D., Cannillo V., Sola A., Chiellini F., Gazzarri M., Migone C., Macroporous Bioglass derived Scaffolds for Bone Tissue Regeneration, Ceram Int 2011, 37, 1575-1585.
[41] Hruby A., Evaluation of Glass-Forming Tendency by means of DTA, Czech J Phys 1972, 22, 1187-1193.
[42] Lara C., Pascual M.J., Duran A., Glass-Forming Ability, Sinterability and Thermal Properties in the System RO-BaO-SiO_2 (R = Mg, Zn), J Non-Cryst Solids 2004, 348, 149-155.
[43] Massera J., Fagerlund S., Hupa L., Hupa M., Crystallization Mechanism of the Bioactive Glasses, 45S5 and S53P4, J. Am. Ceram. Soc. 2012, 95, 607-613.